

Surface Dynamics of A Vanadyl Pyrophosphate Catalyst for *n*-Butane Oxidation to Maleic Anhydride: An In Situ Raman and Reactivity Study of the Effect of the P/V Atomic Ratio

Fabrizio Cavani,^{*[a]} Silvia Luciani,^[a] Elisa Degli Esposti,^[a] Carlotta Cortelli,^[b] and Roberto Leanza^[b]

Dedicated to the Centenary of the Italian Chemical Society

Abstract: This work focused on investigating the effect of the P/V atomic ratio in vanadyl pyrophosphate, catalyst for *n*-butane oxidation to maleic anhydride, on the nature of the catalytically active phase. Structural transformations occurring on the catalyst surface were investigated by means of in situ Raman spectroscopy in a non-reactive atmosphere, as well as by means of steady-state and non-steady-state reactivity tests, in response to changes in the reaction temperature. It was found that the nature of the catalyst surface is affected by the P/V atomic ratio even in the case of small changes in this pa-

rameter. With the catalyst having P/V equal to the stoichiometric value, a surface layer made of α_1 -VOPO₄ developed in the temperature interval 340–400 °C in the presence of air; this catalyst gave a very low selectivity to maleic anhydride in the intermediate *T* range (340–400 °C). However, at 400–440 °C δ -VOPO₄ overlayers formed; at these conditions, the catalyst was moderately active but selective to maleic

anhydride. With the catalyst containing a slight excess of P, the ratio offering the optimal catalytic performance, δ -VOPO₄ was the prevailing species over the entire temperature range investigated (340–440 °C). Analogies and differences between the two samples were also confirmed by reactivity tests carried out after in situ removal and reintegration of P. These facts explain why the industrial catalyst for *n*-butane oxidation holds a slight excess of P; they also explain discrepancies registered in the literature about the nature of the active layer in vanadyl pyrophosphate.

Keywords: butane • maleic anhydride • oxidation • Raman spectroscopy • vanadyl pyrophosphate

Introduction

The selective oxidation of *n*-butane to maleic anhydride (MA), using the vanadyl pyrophosphate (VO)₂P₂O₇ (VPP) catalyst, is the only commercial vapor-phase alkane oxidation process.^[1–5] This reaction, and the unique chemical–physical properties of VPP, have been among the most studied topics in oxidation catalysis in recent decades: initially with the aim of understanding which catalyst peculiarities

make this complex transformation possible, and later on with the aim of improving the process performance.

Many articles discuss the role of different crystalline and/or amorphous compounds in V/P/O (not only VPP, but also other vanadium phosphates) in the complex transformation of the alkane to MA.^[6–13] One controversial aspect of this reaction, however, concerns the nature of the active layer that develops under reaction conditions. While bulk VPP is in all cases assumed to constitute the core of the active phase, the hypotheses formulated differ with regard to the nature of the first atomic layers, that is, those that are in direct contact with the gas phase. It is known that surface reconstruction, especially in the presence of reactive gases, may substantially alter the surface arrangement of atoms as compared to the bulk. However, the identification of the true active layer is a hard task, due to the difficult characterization of the catalytic surface under reaction conditions. Alternative hypotheses either indicate the development of surface amorphous layers which play a direct role in the reaction,^[14–18] or are

[a] Prof. F. Cavani, Dr. S. Luciani, E. D. Esposti
Dipartimento di Chimica Industriale e dei Materiali
ALMA MATER STUDIORUM Università di Bologna
Viale Risorgimento 4, 40136 Bologna (Italy)
Fax: (+39)0512093680
E-mail: fabrizio.cavani@unibo.it

[b] C. Cortelli, R. Leanza
Polynt SpA, Via E. Fermi 51
Scanzorosciate (BG) (Italy)

based on the crystallographic models of VPP, by assuming that specific planes contribute to the reaction pattern,^[19–25] and that the redox process occurs reversibly between VPP and VOPO₄.^[26–28]

An important factor governing the catalytic performance of VPP is the P/V atomic ratio used for catalyst preparation. In fact, it is generally accepted that an excess of P with respect to the stoichiometric requirement (P/V = 1.0) is necessary in order to have a good selectivity for MA.^[19,28] With the aim of finding out whether this parameter may affect the VPP surface characteristics, and then influence the catalytic performance, we investigated the transformations occurring on the surface of two equilibrated catalysts, which contained exclusively VPP but were prepared with different P/V ratio, both by means of in situ Raman spectroscopy in response to variations in the composition of an unreactive gas-phase, and by means of reactivity measurements under both steady-state and non-steady-state conditions. The present paper reports the results of this investigation.

Results

Main characteristics of equilibrated samples: Two VPP-based catalysts were prepared by using V₂O₅ and H₃PO₄ in the amounts needed to obtain a P/V atomic ratio equal to 1.00 and 1.20, respectively (see Experimental Section). Samples will be referred to with the codes P/V1.0 and P/V1.2, regardless of the effective P/V atomic ratio determined analytically (see Table 1). It is worth noting that the P/V ratio

Table 1. Experimental P/V atomic ratio in P/V1.0 and P/V1.2.

| Sample | P/V (SEM-EDX) ^[a] | P/V (XRF) ^[a] | Analytical |
|-------------------------|------------------------------|--------------------------|------------|
| P/V1.0, dried precursor | 0.99 ± 0.02 | 1.02 ± 0.02 | – |
| P/V1.2, dried precursor | 1.08 ± 0.02 | 1.05 ± 0.02 | – |
| P/V1.0, calcined | 0.99 ± 0.02 | – | 1.00 |
| P/V1.2, calcined | 1.05 ± 0.02 | – | 1.06 |

[a] The error reported is the standard deviation calculated after several (at least five) repeated measurements on the same sample.

of the two samples was significantly different. In the case of sample P/V1.2, the effective P/V ratio, ≈ 1.05 , was lower than that used for the preparation of the precursor, but still was systematically higher than that of P/V1.0. In the latter case, the final P/V ratio was the same as that used for the preparation of the precursor.

Figure 1 shows the room-temperature XRD patterns of equilibrated P/V1.0 and P/V1.2 catalysts, that is, of samples downloaded from the reactor after catalytic measurements. Both samples show reflections attributable to VPP; however, traces of δ -VOPO₄ are likely to be present in P/V1.0, as inferred from the very weak reflection at $2\theta = 21.7^\circ$. Nevertheless, the main difference between the two samples concerns their “aspect ratio”, that is, the FWHM (042)/FWHM (200) ratio, equal to 0.81 for P/V1.0 and 0.51 for P/V1.2; the

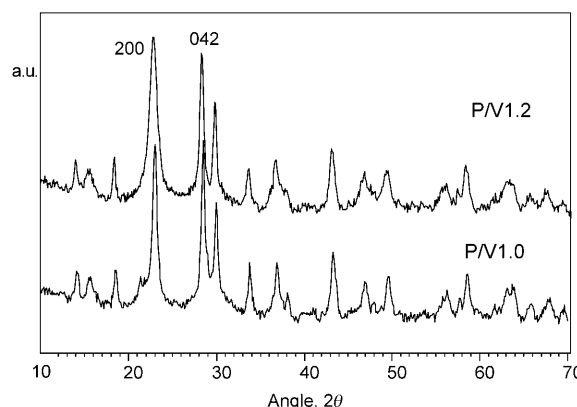


Figure 1. X-ray diffraction patterns of equilibrated P/V1.0 and P/V1.2 samples.

intensity ratio I_{042}/I_{200} being equal to 0.78 and 0.45, respectively. Several authors have pointed out the importance of this morphological parameter.^[23,25,29–31] A lower aspect ratio means a more plate-like morphology, with preferential exposure of {100} crystal faces, (100) being the basal plane of the VPP. This more layered structure is claimed to possess better catalytic performance than the VPP characterized by a lower exposure of the (100) crystallographic plane.^[29–32]

X-ray photoelectron spectroscopy (XPS) of equilibrated samples yielded P/V surface ratios that are not very different for the two samples: 1.76 ± 0.05 and 1.84 ± 0.05 for P/V1.0 and P/V1.2, respectively; this difference did correspond to that found by bulk analytical methods (Table 1). This means that in the latter sample, the excess P with respect to the stoichiometric value is not located on the VPP surface in the form of polyphosphates, a phenomenon that would lead to an XPS P/V atomic ratio considerably higher than the bulk value.

It is worth noting that all literature dealing with XPS on VPP agrees that the P/V surface ratio experimentally found is systematically higher than 1.0, for example, in the 1.5–1.9 range, even for stoichiometric VPP,^[33] possibly due to the presence of V vacancies in the first atomic layers.^[7] In general, however, values in this range are consistent with a number of XPS studies on V/P/O catalysts in which the Schofield sensitivity factors were applied.^[34]

In situ Raman spectroscopy—transformations of VPP in the presence of oxygen or steam:

All in situ Raman spectra were recorded using equilibrated samples. Figure 2 shows the Raman spectra recorded while flowing dry air at different temperatures. In the case of P/V1.0, the spectrum did not show any change during the heating of the sample from room temperature to 380 °C. However, during the isothermal step at 380 °C, after 2 h, some bands attributable to α_1 -VOPO₄ developed (1036 cm^{-1} , and less intense at 540 and 575 cm^{-1} ; Figure 2 top). Then, the intensity of bands attributed to α_1 -VOPO₄ did not increase any more during the isothermal step at 380 °C. When the temperature was raised again from 380 to 440 °C, however, α_1 -VOPO₄ transformed

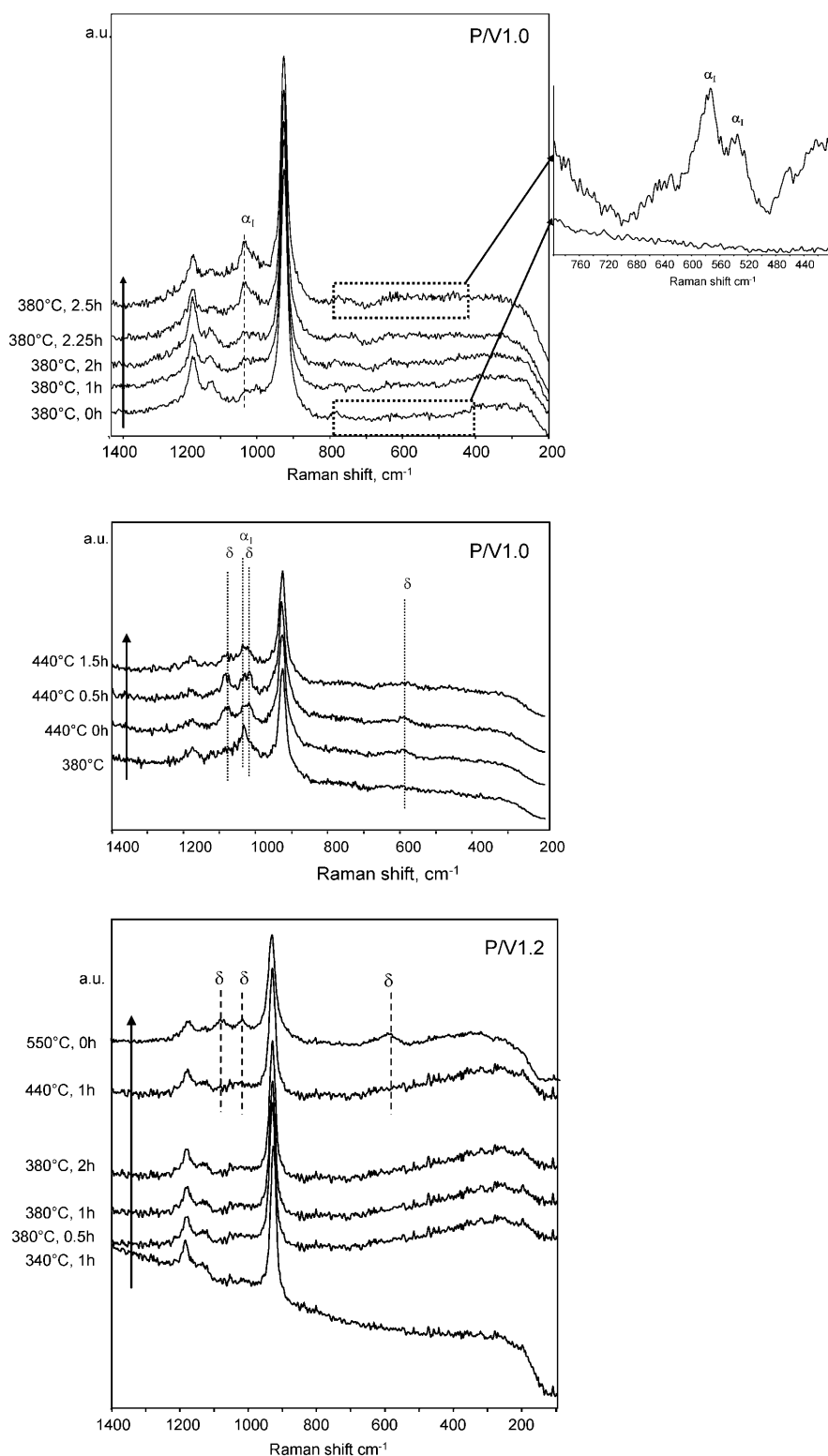


Figure 2. Raman spectra of P/V1.0 (top and center) and P/V1.2 (bottom) recorded in situ in dry air flow, at increasing temperatures and/or time-on-stream. $\alpha_1 = \alpha_1\text{-VOPO}_4$; $\delta = \delta\text{-VOPO}_4$.

into $\delta\text{-VOPO}_4$ (Figure 2 center); in fact, the band at 1036 cm^{-1} decreased, and bands attributable to $\delta\text{-VOPO}_4$ (1080 , 1015 , and 588 cm^{-1}) developed. Conversely, with P/V1.2 there was no modification in the spectrum up to 500°C

(Figure 2 bottom); only at 550°C was the VPP oxidized to $\delta\text{-VOPO}_4$. These experiments clearly demonstrate that the VPP in the two samples shows a different oxidizability in dry air; VPP in P/V1.2 is more stable in an oxidizing environment, and is transformed into $\delta\text{-VOPO}_4$ only at very high temperatures. This agrees with literature findings that an excess of P may stabilize the VPP and hinder its oxidation into V^{V} phosphates.^[19,35]

However, when the treatment of P/V1.2 was carried out under a flow of 10% steam in air, at 380°C , after 1 h a new band at Raman shift 1039 cm^{-1} appeared, thus indicating the formation of a new compound, which was stable for more than 5 h under the conditions used (Figure 3). Then, the band at 1039 cm^{-1} disappeared and bands at 1080 , 1015 , and 588 cm^{-1} formed, all attributable to $\delta\text{-VOPO}_4$; the transformation into $\delta\text{-VOPO}_4$ was even quicker if steam was removed after the development of the band at 1039 cm^{-1} and only air was left (spectra not reported).

Raman bands of V–O–P stretching in V/P/O compounds are usually visible in the spectral range between 1000 and 1100 cm^{-1} , and indeed several of these compounds show bands close to 1040 cm^{-1} .^[36–38] However, when the experiment was carried out under a flow of dry air, dry nitrogen, or even wet nitrogen (10% H_2O), no changes were observed in the spectrum of P/V1.2; in other words, with P/V1.2, at 380°C , VPP transforms into another compound only when in a wet and oxidizing environment. From these experiments, it can be inferred that the band at 1039 cm^{-1} is most likely to be attributable to a V^{V} hydrated phosphate. Notably, this band is one of the most intense in $\text{VOPO}_4 \cdot 2\text{H}_2\text{O}$ (the most intense band is at 950 cm^{-1} , but it is hardly visible, being a shoulder of the P–O stretching

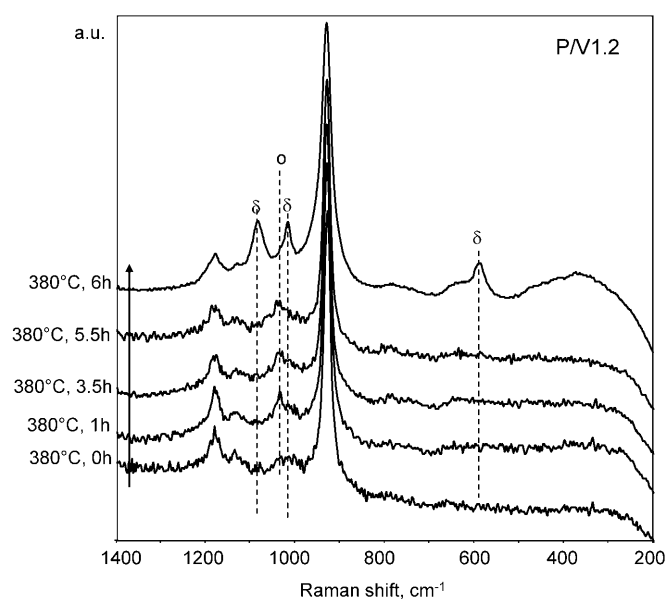


Figure 3. Raman spectra recorded in situ during the isothermal step at 380°C in wet air (10% H₂O) flow. Catalyst = P/V1.2. $\alpha_1 = \alpha_1\text{-VOPO}_4$; $\delta = \delta\text{-VOPO}_4$; $o = \text{VOPO}_4 \cdot 2\text{H}_2\text{O}$.

band in VPP).^[37,38] It may be concluded that the latter compound is formed by the oxidation of VPP in P/V1.2, in the presence of steam. However, after a few hours, in other words, after the transformation of VPP into $\text{VOPO}_4 \cdot 2\text{H}_2\text{O}$ has probably involved a few atomic layers, the hydrated compound is dehydrated into $\delta\text{-VOPO}_4$.

With both samples at 440°C in an air/water feed, VPP was quickly oxidized to $\delta\text{-VOPO}_4$ (Figure 4); typical bands of this compound already appeared after 1.5 h, and their intensity increased during the isothermal step at 440°C. Even when P/V1.0 was first oxidized in dry air at 380°C to $\alpha_1\text{-VOPO}_4$, then brought to 440°C in air, and finally treated at the latter temperature with air/steam, the compound formed was $\delta\text{-VOPO}_4$ (spectra not reported). Therefore, at high temperatures, $\delta\text{-VOPO}_4$ is the compound that is formed by the surface oxidation of VPP, regardless of the presence of either a dry or a wet stream. Similarly, with P/V1.2, the formation of $\delta\text{-VOPO}_4$ at 440°C also occurred in the presence of steam.

These tests demonstrate that the presence of steam in an oxidizing environment plays an important role in transformations occurring at the VPP surface. Steam facilitates the oxidation of VPP in P/V1.2, through the intermediate formation of $\text{VOPO}_4 \cdot 2\text{H}_2\text{O}$. With both samples, however, $\delta\text{-VOPO}_4$ is the preferred compound at high temperature, regardless of the P/V ratio and the presence of steam. It is worth noting that experiments carried out with either dry or wet nitrogen streams showed that samples did not undergo any transformation when treated in the absence of oxygen; VPP was the only stable compound under these conditions.

In situ Raman spectroscopy—reversibility of transformations: Figure 2 shows that in P/V1.0, VPP is oxidized to $\alpha_1\text{-VOPO}_4$

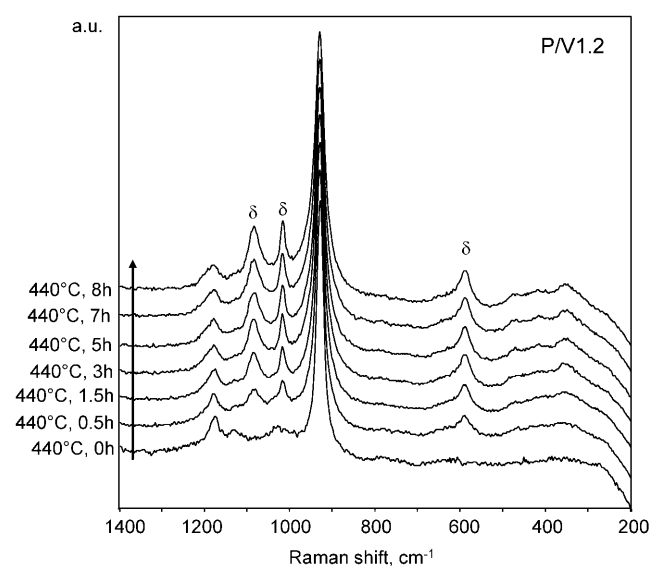
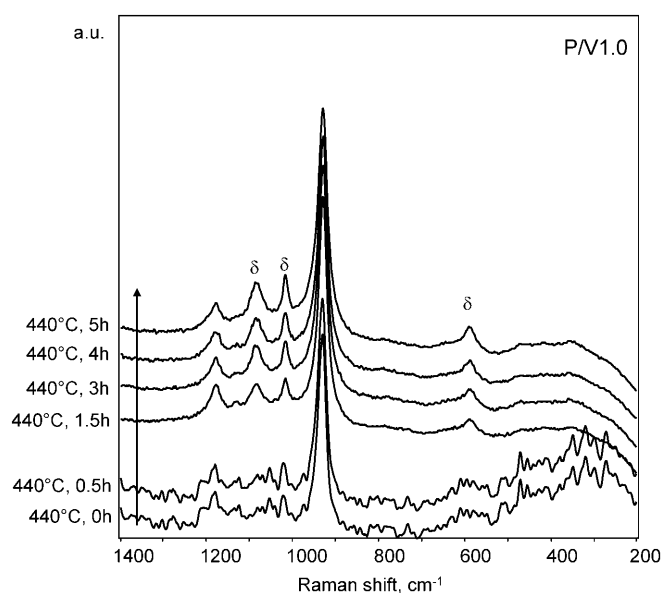


Figure 4. Raman spectra recorded in situ during the isothermal step at 440°C in wet air (10% H₂O) flow. Catalysts: P/V1.0 (top); P/V1.2 (bottom). $\alpha_1 = \alpha_1\text{-VOPO}_4$; $\delta = \delta\text{-VOPO}_4$.

VOPO_4 at 380°C in air, but finally transforms into $\delta\text{-VOPO}_4$ when the temperature is raised to 440°C. When, however, the temperature was decreased again to 380°C, $\delta\text{-VOPO}_4$ transformed back to $\alpha_1\text{-VOPO}_4$ (Figure 5 top). Therefore, the two V^V phosphates interconvert, and the nature of the dominant compound is a function of temperature.

In the case of P/V1.2, when the sample was cooled down from 440 to 380°C in the wet air stream (starting from conditions under which the stable compound on the surface of VPP is $\delta\text{-VOPO}_4$), the hydrated phase $\text{VOPO}_4 \cdot 2\text{H}_2\text{O}$ did not re-form (Figure 5 bottom). Therefore, the transformation of $\text{VOPO}_4 \cdot 2\text{H}_2\text{O}$ into $\delta\text{-VOPO}_4$ is not reversible. This also agrees with the spectra reported in Figure 3; in fact, experiments at 380°C showed that $\text{VOPO}_4 \cdot 2\text{H}_2\text{O}$ finally trans-

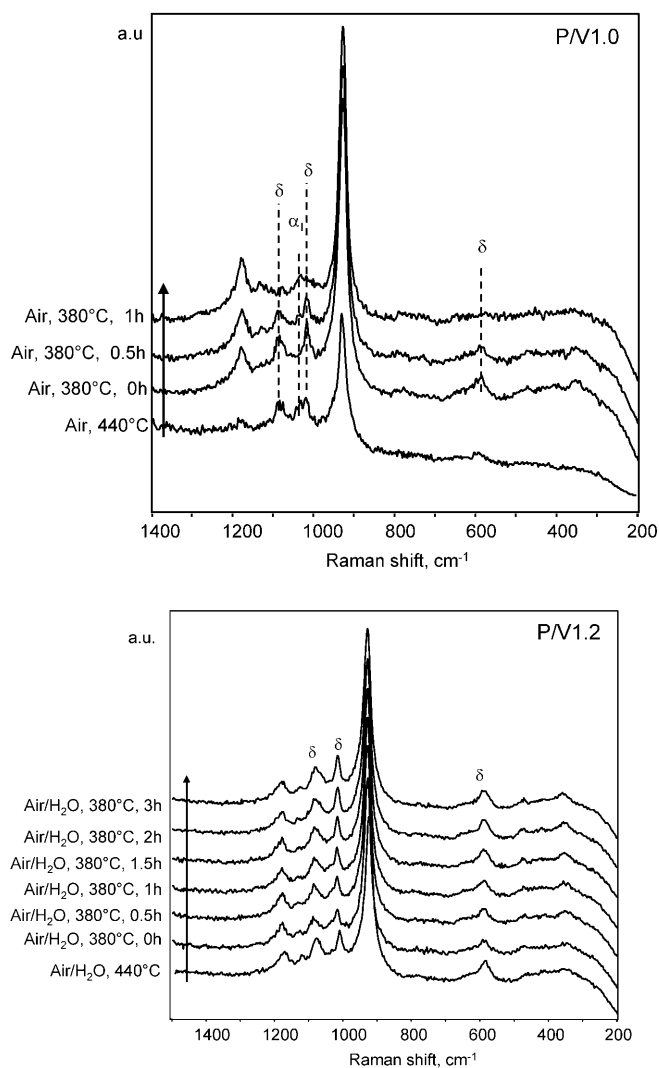


Figure 5. Raman spectra recorded in situ by cooling from 440 to 380 °C in dry air flow (top, catalyst P/V1.0), and by cooling in wet air (10% H₂O) flow (bottom, catalyst P/V1.2). $\alpha_1 = \alpha_1\text{-VOPO}_4$; $\delta = \delta\text{-VOPO}_4$.

formed into $\delta\text{-VOPO}_4$ after a prolonged exposure to the wet air flow. It may be concluded that $\text{VOPO}_4 \cdot 2\text{H}_2\text{O}$ is not a stable compound, and is dehydrated to $\delta\text{-VOPO}_4$ at both 380 and 440 °C, even in the presence of steam.

Steady-state reactivity tests: Figure 6 shows the catalytic performance of equilibrated catalysts at steady state. The two samples exhibited quite different behaviors. P/V1.2 showed the expected increase in *n*-butane conversion when the reaction temperature was raised, and a slight decline in selectivity towards MA.

Conversely, P/V1.0 showed an anomalous behavior. In fact, the conversion rapidly increased in the 340–360 °C temperature range, then remained approximately constant ($\approx 50\%$) up to 400 °C, and finally increased again. Correspondingly, the selectivity towards MA fell dramatically at 340 °C, reaching a minimum value of 27% at 360 °C, and then increased again up to 68%, the maximum value being

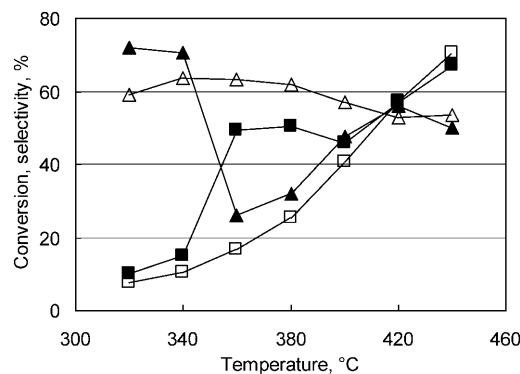


Figure 6. *n*-Butane conversion (■ □) and selectivity to MA (▲ △) as functions of temperature, for P/V1.0 (full symbols) and P/V1.2 (open symbols).

obtained at 440 °C. The following observations are especially worth noting:

- 1) This behavior was fully reproduced when the reaction temperature was increased and then decreased several times; in other words, the observed phenomena were not due to some effects attributable to irreversible changes in catalyst characteristics.
- 2) The two samples showed very similar performance in the temperature ranges of 320–340 °C and 400–440 °C, but they gave quite different performances in the intermediate temperature range, 340–400 °C.
- 3) The fall of selectivity towards MA shown by P/V1.0 at above 340 °C was not simply due to the anomalous rise in conversion. In fact, it must be noted that a selectivity of 27% is too low to be attributed solely to the enhanced contribution of consecutive combustions.

All this evidence suggests that the behavior of P/V1.0 is related to a modification in the surface characteristics under reaction conditions; in the intermediate temperature range, a very active but poorly selective active layer develops, which is different not only from the one forming at either low or high temperature (selective and moderately active), but also from the one that develops with P/V1.2 in the intermediate temperature range. Therefore, the active layers of the two catalysts are probably similar, or, at least, offer similar performances in the low- and high-temperature intervals, whereas they are different in the intermediate-temperature ranges. In conclusion, it appears that reactivity tests have a clear correspondence with in situ Raman experiments, although the latter were carried out in a non-reactive atmosphere. In order to confirm these hypotheses, reactivity tests under non-steady-state conditions were carried out.

Non-steady-state reactivity tests—how catalysts react to temperature changes: Figure 7 summarizes the results of reactivity tests carried out with P/V1.0 (top) and P/V1.2 (bottom), obtained in response to modifications in the reaction temperature. The reaction was first carried out at

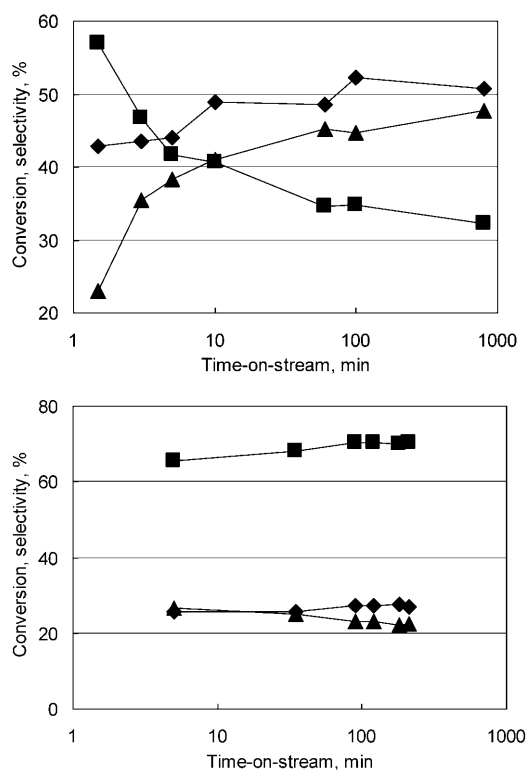


Figure 7. Conversion of *n*-butane (◆), selectivity to MA (■), and CO_x (▲), as functions of time-on-stream at 380°C after i) reaction at 440°C, ii) cooling in N₂ down to 380°C, and iii) feed of the reaction stream again. Catalysts P/V1.0 (top), P/V1.2 (bottom).

440°C; then the reaction stream was interrupted, and the catalyst was cooled down to 380°C in nitrogen flow; finally, the reaction stream was fed again, and results were recorded.

The results summarized in this figure show the conversion of *n*-butane and the selectivity towards the main products, MA and CO_x, as functions of time-on-stream after the start-up of the reaction feed. This test is aimed at checking whether the active layer that develops in the reaction environment at 440°C is the same as that which forms at 380°C. In fact, if the active layer is the same, no major modification of its characteristics is expected in the presence of the reactive atmosphere when the reaction temperature is changed; therefore, the catalyst should show no variation in catalytic performance when the reaction is started again at 380°C. Conversely, if the active layer at the two temperatures is not the same, the one that had formerly developed at 440°C is going to be modified when the feed stream is fed again at 380°C; in fact, in this case there would be a new composition for the active layer, in equilibrium with the gas phase at those specific conditions. Therefore, in this case, a progressive modification of reactivity is expected, in parallel with the passage from the former, high-temperature active layer to the new, intermediate-temperature active layer.

Figure 7 (top) shows that this was indeed the case for P/V1.0. The catalyst took several hours to reach the new steady performance after the start-up of the reaction feed at

380°C. This means that the active layer that develops in the reaction environment at 380°C is different from that formerly developed at 440°C, and that the latter is less active but remarkably more selective than the former. The opposite occurred when the operation was carried out in reverse, that is, increase in temperature of nitrogen from 380 to 440°C, and start of the feed again. These results confirm that the behavior shown in Figure 6 (tests at steady-state conditions) was due to the modification of the active layer characteristics in the reaction environment that occurred when the temperature was changed. It is worth mentioning that the time needed to reach the steady performance (a few hours) is compatible with the changes recorded by means of *in situ* Raman experiments.

Conversely, in the case of P/V1.2 (Figure 7 [bottom]) the catalytic performance showed only minor changes when the temperature was changed; this indicates that, for this catalyst, the nature of the active layer is similar at both 380 and 440°C.

In situ modification of the P/V ratio: Catalytic tests highlight the importance of the P/V ratio in VPP, and indicate that small differences in this parameter may have remarkable effects on reactivity. In order to confirm the role of phosphorus, we performed tests aimed at its *in situ* removal, in the form of volatile esters, from the catalyst surface, and then at the reintegration of the P formerly removed. The catalytic performance of the sample was checked after both P removal and reintegration, and compared with the performance of the original equilibrated catalyst.

Specifically, P/V1.2 was first heated in a mixture of *n*-butane and air up to 440°C; then the reagents stream was interrupted and a flow of 3 mol % steam in He was fed. The purpose of this treatment was to cause the hydrolysis of the VPP surface.^[12] After 2 h, the steam feed was stopped and the temperature was decreased to 380°C under a He flow; then, a mixture of 0.8 mol % ethanol in He was fed for 1 h. Under these conditions, the free phosphoric acid is expected to react with ethanol to generate volatile ethyl esters (boiling temperature 215°C). In fact, the analysis of the used catalyst confirmed that the bulk P/V ratio had decreased by 8–9% (as determined by scanning electron microscope/energy dispersive X-ray (SEM-EDX) analysis). After that, the *n*-butane/air mixture was fed again at 380°C and reactivity was checked and compared with that of the catalyst before treatment. Finally, the reactants stream was stopped again and a feed of approximately 1 mol % of alkyl phosphite or phosphate vapors in He (obtained by saturation of the He flow by bubbling in the liquid maintained at 0°C) was fed for 1 h; the catalytic performance was checked both at an intermediate step, after 20 min, and at the end of the treatment. The analysis of the used catalyst, after catalytic measurements, confirmed that the original level of P had been recovered. Figure 8 summarizes all the results obtained, showing the relative variation in conversion and selectivity to MA and by-products (all values referring to the initial corresponding values for the equilibrated, untreated catalyst

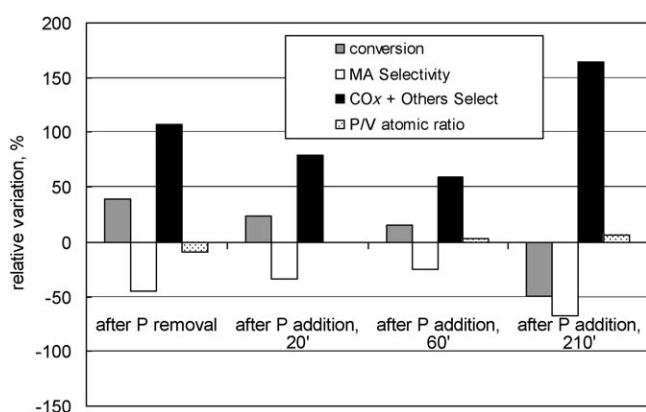


Figure 8. Relative variation of conversion, selectivity to MA, and selectivity to CO_x + others (all referring to the corresponding initial values shown by the equilibrated, untreated catalyst), after in situ removal of P, and after in situ reintegration of P (see text for details of treatment).

having excess P). It is shown that the removal of P led to an increase in catalyst activity, whereas the selectivity for MA decreased remarkably, with a corresponding increase in the selectivity for by-products. In practice, the behavior of the catalyst had become more similar to that of sample P/V1.0. After this, the in situ treatment with the P-containing compound allowed the reintegration of P and the recovery, at least in part, of the initial catalytic behavior of the P/V1.2 catalyst. It is worth noting that when the treatment for P reintegration was prolonged for 210 min, the P/V ratio increased further; after that, however, the catalyst showed a very poor catalytic performance, with low conversion and bad selectivity to MA. Therefore, an excessive amount of P accumulated on the catalyst surface led to a worse catalytic performance.

In a further analogy with the behavior of the untreated catalysts, the catalytic performance of the sample at 440 °C did not change, after both the P removal and P reintegration treatments. In fact, Figure 6 shows that P/V1.0 and P/V1.2 had similar performances at high temperature; therefore removal of P from P/V1.2 was not expected to cause any change in performance.

Discussion

The effect of small P/V differences on morphological features of samples:

One relevant structural difference between the equilibrated P/V1.0 and P/V1.2 samples concerns the so-called aspect ratio, that is a measure providing information on the preferential exposure of the (100) crystallographic plane of VPP. This parameter has major implications on catalytic performance, and although some discrepancy exists in literature, it is generally agreed that: 1) samples with a more platelet-like morphology perform better than samples having a bulkier morphology,^[39] and that 2) catalysts with a well-ordered stacking of the (200) planes (lower I_{042}/I_{200} ratio) offer the best performance, in terms of both activity

and selectivity.^[25] This latter feature has been attributed to the fact that the oxidation of the {100} faces leads to the development of selective γ - or δ -VOPO₄ phases, whereas side faces are oxidized to unselective compounds, α - or β -VOPO₄.^[32,40,41]

Literature reports that the morphology of calcined VPP may be greatly affected by procedures adopted for both the catalyst preparation and the thermal transformation of the precursor into VPP.^[30,31,42–44] Variations in morphological parameters have been attributed either to the presence of lattice strains or microcracking,^[45,46] or to the existence of polytypes characterized by differences in the relative orientation of adjacent dimeric vanadium polyhedra.^[23,47] Torardi et al.^[48] have noted that the final VPP is made up of highly oriented microcrystals, and that the large contraction of the atomic structure in the direction perpendicular to the basal plane that occurs by transformation of the precursor induces cracks and voids within the crystal. In fact, the dehydration of the precursor yields VPP particles constituted by a great number of slightly misoriented, small crystallites, showing mosaic texture, with generation of intercrystallite boundaries, which are disorganized areas.^[49] High temperatures of calcination lead to a change of morphology, and to transformation from a plate morphology into prismatic VPP, due to fragmentation and sintering of the initial plates. These phenomena also occur with a relevant variation of the particle aspect ratio. It was shown that the mosaic microstructure gives the highest yield of MA, and it was also proposed that the defect areas located between the {100} mosaic facets may be sites for the location of additional species playing a role in catalytic oxidation.^[29]

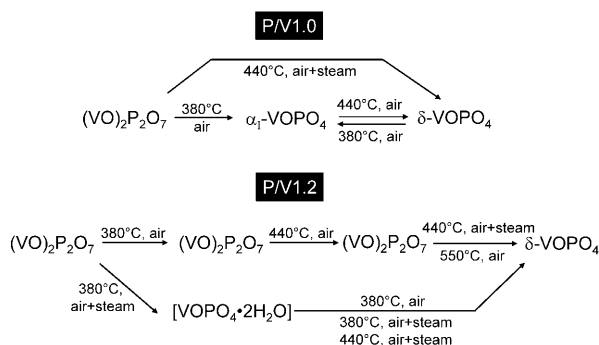
Our P/V1.0 and P/V1.2 samples were prepared by adopting the same procedure and thermal treatment, and only show a slight difference in the amount of P. In fact, the two samples were prepared using different P/V atomic ratios of 1.00 and 1.20; however, the precursor VOHPO₄·0.5H₂O was carefully washed with isobutanol to remove any excess P that may have been adsorbed on the precipitate. Finally, the P/V ratio determined in calcined and equilibrated samples was equal to 1.00 ± 0.02 and 1.05 ± 0.02 for P/V1.0 and P/V1.2, respectively. It is worth noting that the difference in the P/V atomic ratio between the two samples also corresponds to the difference determined by XPS. This means that the excess of P (5% with respect to the stoichiometric requirement) in P/V1.2 is not present in the form of polyphosphates dispersed over the surface of VPP crystals. We propose here that the slight excess of P, holding such a relevant role in the catalytic performance, may be located in defective areas of the more platy samples, being uniformly dispersed in the entire bulk of VPP particles; this may explain the fact that differences of the P/V ratio in the two samples are similar when determined either by XPS or by bulk analytical methods. This hypothesis is also supported by the evidence that one reason for catalyst deactivation in the industrial reactor is the loss of excess P; catalyst ageing occurs with the concomitant increase of VPP crystallinity, and increase of the FWHM (042)/FWHM (200) aspect ratio and

I_{042}/I_{200} intensity ratio. On the other hand, due to the fact that the methods adopted for the preparation of our samples were identical except for the different P/V atomic ratio used, it is likely that this excess P is indeed responsible for the different morphology of the samples.

The dynamics of V/P/O catalysts, as a function of temperature and catalyst composition: Our in situ Raman experiments show that:

- 1) With P/V1.2, the VPP is stable; it is not oxidized by air at mild temperature, and is transformed into δ -VOPO₄ only at $T > 500^\circ\text{C}$. In the presence of steam, however, VPP is transformed into δ -VOPO₄ at both 380 and 440 °C, through the intermediate formation of VOPO₄·2H₂O. Lastly, δ -VOPO₄ is the stable V phosphate formed on the surface of VPP over the entire temperature range, from 380 to 440 °C, under an atmosphere containing both oxygen and steam.
- 2) With P/V1.0, VPP is more easily oxidizable, and even at 380 °C it is transformed into α_1 -VOPO₄. This compound is easily hydrolyzable into VO_y + (PO₄)_n.^[12] At 440 °C, the stable compound, both in the presence and in the absence of steam, is δ -VOPO₄. Remarkably, if the temperature decreases again from 440 down to 380 °C, and steam is removed, δ -VOPO₄ reverts to α_1 -VOPO₄.

Scheme 1 summarizes the results of in situ Raman experiments at 380 and 440 °C. The main difference between the two samples concerns the nature of the compound formed



Scheme 1. A summary of the results from in situ Raman spectroscopy measurements.

on the surface of VPP at 380 °C. With P/V1.0, the compound formed in the presence of air is α_1 -VOPO₄, which may eventually be hydrolyzed into VO_y + (PO₄)_n in the presence of steam.^[12] With P/V1.2, the stable compound on the VPP surface at 380 °C is δ -VOPO₄. At high temperature, however, the two samples have a similar behavior, and the compound formed by surface oxidation of VPP is δ -VOPO₄.

Relationships between catalytic tests and in situ Raman characterization: Raman characterization demonstrates that

the different catalytic behaviors shown by P/V1.0 and P/V1.2 may be due to differences in the nature of the active layer that develops under reaction conditions. In the case of P/V1.2, the active layer formed at both intermediate and high temperatures is the same, whereas with P/V1.0 it is different. This is the reason why, with this catalyst: 1) the catalytic performance at the two temperature levels is quite different (Figure 6), and 2) the catalyst takes a few hours to re-equilibrate and reach a stable performance when the temperature is changed (Figure 7).

In the literature, the positive effect of a slight excess of P on catalytic performances has long been known. While P/V ratios much higher than 1.0 lead to the development of vanadyl metaphosphate VO(PO₃)₂, which is quite inactive in the reaction,^[25,50] no formation of vanadyl metaphosphate is observed in the case of P/V ratios between 1.1 and 1.2, and this catalyst offers the best performance.^[51] More specifically, it was reported that the overall conversion of *n*-butane was the highest for P/V close to one, whereas the highest selectivity towards MA was registered for the highest P/V ratio, for example, P/V of 1.07, a value that agrees with our experimental observations. In the literature, various authors have investigated the role of VPP defectivity on catalytic performance.^[52–54] Cornaglia et al.,^[52] for instance, found that a greater defectivity in non-equilibrated VPP catalysts led to a more active but less selective catalyst. However, no clear relationship was established between the VPP defectivity and the P/V atomic ratio.

Although our in situ Raman experiments were not carried out in a reactive atmosphere, there are apparent analogies between the results of both these experiments and catalytic tests. Raman experiments lead to the conclusion that in P/V1.0, the nature of the surface that develops over the VPP is different from the one formed at 440 °C, whereas with P/V1.2 the VPP surface has similar characteristics at the two different temperature levels. Even more remarkably, the surface of VPP for the two catalysts is very different at 380 °C (that is the temperature at which their catalytic behavior is very different too), whereas it is similar at 440 °C (the temperature at which the two samples offer a rather similar catalytic behavior). This result suggests that the active layer offering the best selectivity towards MA is δ -VOPO₄, and that with both catalysts the latter is formed by the oxidation of VPP at high temperature, especially in the presence of steam, whereas at intermediate temperature it is formed only in P/V1.2, and in the presence of steam. This also agrees with indications in the literature concerning the role of δ -VOPO₄ in *n*-butane oxidation;^[55–57] it cannot be ruled out, however, that in the presence of hydrocarbon the V^V phosphate is readily reduced back to VPP and that, under a reactive atmosphere, the surface of the catalyst is reduced on average, if the re-oxidation of V is the rate-limiting step of the reaction.

The less selective, but more active, surface layer formed in the intermediate *T* range in P/V1.0 is probably made of a mixture of α_1 -VOPO₄ and VO_y + (PO₄)_n.

Conclusions

The effect of the P/V atomic ratio on the nature of the compounds formed on the surface of VPP, both in the presence of air and dependent on temperature, was investigated by means of in situ Raman spectroscopy. It was found that a dynamic equilibrium between various compounds is reached on the VPP surface. In the intermediate T range (340–400 °C) the main components are α_1 -VOPO₄ and δ -VOPO₄. The former develops with the catalyst having the stoichiometric P/V bulk ratio; the latter with the catalyst having a slight excess of P, but only in the presence of steam. For both catalysts, however, the prevailing compound at high temperature (400–440 °C) is δ -VOPO₄. Moreover, in P/V1.0 the transformation of α_1 -VOPO₄ into δ -VOPO₄ is reversible: the two compounds interconvert.

These results were used to interpret the catalytic behavior observed experimentally: under conditions giving the prevailing formation of δ -VOPO₄, both catalysts offered the optimal catalytic performance, with high selectivity towards MA and moderate activity in n -butane conversion. With the stoichiometric catalyst and at intermediate reaction temperature, that is, under conditions leading to the formation of α_1 -VOPO₄, the selectivity towards MA was very low, whereas the catalytic activity was very high (Figure 9).

| | |
|------------------------------------|---------------------|
| δ -VOPO ₄ | |
| Moderately active, selective | |
| P/V > 1.0 | 340 °C < T < 440 °C |
| P/V = 1.0 | 400 °C < T < 440 °C |
| P/V = 1.0 340 °C < T < 400 °C | |
| Very active, non selective | |
| α_1 -VOPO ₄ | |

Figure 9. A summary of the effect of the P/V atomic ratio in VPP on both the catalytic performance and the nature of the active layer.

The effect observed experimentally explains why the industrial catalyst for n -butane oxidation holds a slight excess of P; it also explains the discrepancies found in the literature about the nature of the active layer in VPP. These discrepancies can be attributed to small differences in the P/V ratio of samples. Here, it is also proposed that the small excess of P is adsorbed on the vanadyl orthophosphate during the synthetic step, and, lastly, located in the defective areas of mosaic crystals that form VPP, being responsible in the end for differences in morphology observed experimentally among samples with different P/V atomic ratios.

Experimental Section

Synthesis: For the synthesis of the VPP precursor, VOHPO₄·0.5H₂O, the “organic procedure” was adopted. The precursor was obtained by heating under reflux V₂O₅ (10.04 g, Sigma–Aldrich, purity 99.6%) and 100%

H₃PO₄ (Sigma–Aldrich, purity ≥98%, either 10.94 g [P/V=1.00] or 13.13 g [P/V=1.20]) in isobutanol (120 mL, Sigma–Aldrich purity ≥99.5%) for 6 h ($T=110$ °C). After filtration, the light blue precipitate was first washed with isobutanol (20 mL) and acetone (20 mL), to remove the excess phosphoric acid. The washed precipitate was then dried at 120 °C for 12 h, in static air, and lastly thermally treated according to the following procedure: a) pre-calcination step in flowing air, with temperature gradient from room temperature up to 300 °C; then isothermal step at 300 °C in air for 6 h; b) thermal treatment in flowing N₂, with temperature gradient up to 550 °C, and final isothermal step at the latter temperature for 6 h; and c) equilibration under reaction conditions for 100 h. Equilibration leads to various transformations in calcined V/P/O catalysts, including: 1) the crystallization of amorphous components, if any were present in the fresh catalysts, to VPP; 2) the reduction of bulk VOPO₄ to VPP; 3) the oxidation of V^{III} phosphates to VPP; and 4) the increase in the crystallinity of VPP.

Raman spectroscopy: In situ Raman analyses were performed using a Renishaw 1000 instrument equipped with a Leica DMLM microscope, argon-ion laser source (514 nm), and a commercial Raman cell (Linkam Instruments TS1500). A small amount of catalyst (1–5 mg) was loaded into the ceramic crucible of the cell. First, the spectrum was recorded at room temperature, then the temperature was increased up to the desired value (heating rate 50 min⁻¹), while recording spectra at intermediate temperatures, and finally maintained in isothermal conditions for a few hours at the final temperature. A continuous flow of GC-grade air or N₂ (flow rate 50 Ncm³min⁻¹) was fed to the cell from the very beginning of each experiment. A saturator allowed the feeding of steam-saturated air or nitrogen; the change in the saturator temperature made it possible to vary the partial pressure of water, from 0.03 to 0.10 bar. In situ spectra were recorded for “equilibrated” catalysts (samples that had been preliminarily treated in the reactive phase at 400 °C for 100 h reaction time).

X-ray photoelectron spectra (XPS): XPS were recorded with a VG ESCALAB 220 XL spectrometer equipped with a monochromatic Al_{K α} ($E=1486.6$ eV) X-ray source, using the C 1s peak (285.0 eV) as a reference. Spectra were collected with a pass energy of 40 eV, using the electromagnetic lens mode low-energy electron flood gun (6 eV) for charge compensation effect; O 1s/V 2p, C 1s, and P 2p core levels were recorded.

X-ray diffraction (XRD): XRD patterns were recorded using the Philips PW 1710 apparatus, with Cu_{K α} ($\lambda=1.5406$ Å) as a radiation source.

Chemical analysis: The chemical analysis of samples was performed as follows. The equilibrated sample was dissolved in concentrated fuming sulfuric acid. Then its V content was determined by titration of V^V with a Mohr salt solution (Fe^{II}), and V^{IV} was determined by titration with a KMnO₄ 0.1 N solution. Phosphorus was determined gravimetrically as quinoline molybdophosphate.

Catalytic tests were carried out in a quartz continuous-flow reactor, loading 0.8 g of catalyst and feeding 1.7% n -butane and 17% oxygen (remainder N₂). Overall GHSV was 2160 h⁻¹. Products were analyzed online by sampling a volume of the outlet gas stream and injecting into a gas chromatograph equipped with an HP-1 column for the separation of C₄ hydrocarbons, formaldehyde, acetic acid, acrylic acid, and MA. A Carbosieve SII column was used for the analysis of oxygen, CO, and CO₂.

Acknowledgements

Prof. Elisabeth Bordes-Richard, Université des Sciences et Technologies de Lille, is acknowledged for XPS measurements.

- [1] N. Ballarini, F. Cavani, C. Cortelli, S. Ligi, F. Pierelli, F. Trifirò, C. Fumagalli, G. Mazzoni, T. Monti, *Top. Catal.* **2006**, *38*, 147.
- [2] P. Arpentiner, F. Cavani, F. Trifirò, *The Technology of Catalytic Oxidations*, **2001**, Editions Technip, Paris.
- [3] S. Albonetti, F. Cavani, F. Trifiro, *Catal. Rev. Sci. Eng.* **1996**, *38*, 413.
- [4] J. C. Volta, *C.R. Acad. Sci. Paris* **2000**, *3*, 717.
- [5] E. Bordes, *Top. Catal.* **2001**, *15*, 131.

- [6] F. Richter, H. Papp, T. Gotze, G. U. Wolf, B. Kubias, *Surf. Interface Anal.* **1998**, *26*, 736.
- [7] P. Delichère, K. E. Bere, M. Abon, *Appl. Catal. A* **1998**, *172*, 295.
- [8] L. M. Cornaglia, E. A. Lombardo, *Appl. Catal. A* **1995**, *127*, 125.
- [9] H. Bluhm, M. Hävecker, E. Kleimenov, A. Knop-Gericke, A. Liskowski, R. Schlögl, D. S. Su, *Top. Catal.* **2003**, *23*, 99.
- [10] M. Hävecker, A. Knop-Gericke, H. Bluhm, E. Kleimenov, R. W. Mayer, M. Fait, R. Schlögl, *Appl. Surf. Sci.* **2004**, *230*, 272.
- [11] M. Hävecker, R. W. Mayer, A. Knop-Gericke, H. Bluhm, E. Kleimenov, A. Liskowski, D. S. Su, R. Follath, F. G. Requejo, D. F. Ogle-tree, M. Salmeron, J. A. Lopez-Sanchez, J. K. Bartley, G. J. Hutchings, R. Schlögl, *J. Phys. Chem. B* **2003**, *107*, 4587.
- [12] Z. Y. Xue, G. L. Schrader, *J. Phys. Chem. B* **1999**, *103*, 9459.
- [13] V. V. Guliants, S. A. Holmes, J. B. Benziger, P. Heaney, D. Yates, I. E. Wachs, *J. Mol. Catal. A* **2001**, *172*, 265.
- [14] H. Berndt, K. Buker, A. Martin, A. Brückner, B. Lücke, *J. Chem. Soc. Faraday Trans.* **1995**, *91*, 725.
- [15] A. Brückner, A. Martin, N. Steinfeldt, G. U. Wolf, B. Lücke, *J. Chem. Soc. Faraday Trans.* **1996**, *92*, 4257.
- [16] A. Brückner, B. Kubias, B. Lücke, *Catal. Today* **1996**, *32*, 215.
- [17] M. Ruitenbeek, A. J. van Dillen, A. Barbon, E. E. van Fassen, D. C. Koningsberger, J. W. Geus, *Catal. Lett.* **1998**, *55*, 133.
- [18] A. Brückner, A. Martin, B. Kubias, B. Lücke, *J. Chem. Soc. Faraday Trans.* **1998**, *94*, 2221.
- [19] F. Cavani, F. Trifirò, *Chemtech* **1994**, *24*, 18.
- [20] I. E. Wachs, J. M. Jehng, G. Deo, B. M. Weckhuysen, V. V. Guliants, J. B. Benziger, *Catal. Today* **1996**, *32*, 47.
- [21] E. Bordes, J. W. Johnson, A. Raminosona, P. Courtine, *Mater. Sci. Monograph. B* **1985**, *28*, 887.
- [22] P. A. Agaskar, L. DeCaul, R. K. Grasselli, *Catal. Lett.* **1994**, *23*, 339.
- [23] R. Ebner, M. R. Thompson, *Catal. Today* **1993**, *16*, 51.
- [24] V. V. Guliants, J. B. Benziger, S. Sundaresan, N. Yao, I. E. Wachs, *Catal. Lett.* **1995**, *32*, 379.
- [25] V. V. Guliants, J. B. Benziger, S. Sundaresan, I. E. Wachs, J. M. Jehng, J. E. Roberts, *Catal. Today* **1996**, *28*, 275.
- [26] G. Koyano, T. Okuhara, M. Misono, *J. Am. Chem. Soc.* **1998**, *120*, 767.
- [27] G. Koyano, T. Saito, M. Misono, *J. Mol. Catal. A* **2000**, *155*, 31.
- [28] J. Ziolkowski, E. Bordes, *J. Mol. Catal.* **1993**, *84*, 307.
- [29] N. Duvauchelle, E. Bordes, *Catal. Lett.* **1999**, *57*, 81.
- [30] E. Bordes, P. Courtine, *J. Catal.* **1979**, *57*, 236.
- [31] I. Matsuura, M. Yamazaki, *Stud. Surf. Sci. Catal.* **1990**, *55*, 563.
- [32] E. Bordes, *Catal. Today* **1993**, *16*, 27.
- [33] L. O'Mahony, T. Curtin, J. Henry, D. Zemlyanov, M. Mihov, B. K. Hodnett, *Appl. Catal. A* **2005**, *285*, 36.
- [34] L. O'Mahony, T. Curtin, D. Zemlyanov, M. Mihov, B. K. Hodnett, *J. Catal.* **2004**, *227*, 270.
- [35] G. Centi, F. Trifirò, J. R. Ebner, V. Franchetti, *Chem. Rev.* **1988**, *88*, 55.
- [36] F. Benabdelouahab, R. Olier, M. Ziyad, J. C. Volta, *J. Catal.* **1995**, *157*, 687.
- [37] F. Benabdelouahab, R. Olier, N. Guillaume, F. Lefebvre, J. C. Volta, *J. Catal.* **1992**, *134*, 151.
- [38] F. Benabdelouahab, J. C. Volta, R. Olier, *J. Catal.* **1994**, *148*, 334.
- [39] T. Okuhara, M. Misono, *Catal. Today* **1993**, *16*, 61.
- [40] G. Koyano, T. Okuhara, M. Misono, *Catal. Lett.* **1995**, *32*, 205.
- [41] G. Koyano, F. Yamaguchi, T. Okuhara, M. Misono, *Catal. Lett.* **1996**, *41*, 149.
- [42] I. Matsuura, *Catal. Today* **1993**, *16*, 123.
- [43] E. Bordes, P. Courtine, *J. Chem. Soc. Chem. Commun.* **1985**, 294.
- [44] E. Bordes, J. W. Johnson, P. Courtine, *J. Solid State Chem.* **1984**, *55*, 270.
- [45] H. S. Horowitz, C. M. Blackstone, A. W. Sleight, G. Teufer, *Appl. Catal.* **1988**, *38*, 193.
- [46] P. T. Nguyen, A. W. Sleight, N. Roberts, W. W. Warren, *J. Solid State Chem.* **1996**, *122*, 259.
- [47] J. R. Ebner, M. R. Thompson, *Stud. Surf. Sci. Catal.* **1991**, *67*, 31.
- [48] C. C. Torardi, Z. G. Li, H. S. Horowitz, W. Liang, M. H. Whangbo, *J. Solid State Chem.* **1995**, *119*, 349.
- [49] N. Duvauchelle, E. Kesteman, F. Oudet, E. Bordes, *J. Solid State Chem.* **1998**, *137*, 311.
- [50] F. Cavani, G. Centi, F. Trifirò, *Appl. Catal.* **1985**, *15*, 151.
- [51] B. K. Hodnett, Ph. Permanné, B. Delmon, *Appl. Catal.* **1983**, *6*, 231.
- [52] L. M. Cornaglia, C. Caspani, E. A. Lombardo, *Appl. Catal.* **1991**, *74*, 15.
- [53] M. T. Sananes Schulz, A. Tuel, G. J. Hutchings, J. C. Volta, *J. Catal.* **1997**, *166*, 388.
- [54] K. Ait-Lachgar, M. Abon, J. C. Volta, *J. Catal.* **1997**, *171*, 383.
- [55] N. H. Batis, A. Ghorbel, J. C. Vedrine, J. C. Volta, *J. Catal.* **1991**, *128*, 248.
- [56] Y. Zhanglin, M. Forissier, R. P. Sneed, J. C. Vedrine, J. C. Volta, *J. Catal.* **1994**, *145*, 256.
- [57] C. J. Kiely, S. Sajip, I. J. Ellison, M. T. Sananes, G. J. Hutchings, J. C. Volta, *Catal. Lett.* **1995**, *33*, 357.

Received: July 21, 2009

Published online: December 9, 2009